PREDICTION OF RESIDUAL STRESS INDUCED BY HIGH-FREQUENCY MECHANICAL IMPACT TREATMENT

Takeshi HANJI*, Kazuo TATEISHI, Suguru KANO and Masaru SHIMIZU
Nagoya University (Aichi, Japan, hanji@civil.nagoya-u.ac.jp)

ABSTRACT: In this study, a method for predicting residual stress introduced by high-frequency mechanical impact (HFMI) was investigated using kinetic energy of an accelerated indenter. Steel plates of different grades were treated by a high-frequency impact treatment device under different treatment conditions (such as intensity of impact, number of passes, and treatment length). In addition, the motion of the HFMI indenter was recorded using a high-speed camera during the treatment, and a simple calculation method for the kinetic energy applied to steel plates was proposed. The results confirmed that the compressive residual stress introduced to the steel plates correlated closely with the calculated kinetic energy. In addition, experiments demonstrated that the energy-based residual stress prediction is applicable to a longitudinal attachment welded joint with sufficient accuracy.

Keywords: high-frequency mechanical impact (HFMI) treatment, residual stress, kinetic energy, groove profile, fatigue strength enhancement

1. INTRODUCTION

Tensile residual stress created by the joining process has a negative effect on the fatigue strength of welded joints. High-frequency mechanical impact (HFMI) treatment is one technique to enhance the fatigue strength of welded joints, and it can reduce the tensile residual stress and introduce compressive residual stress at a weld toe [1]. Numerous studies on HFMI treatment have been performed using various types of HFMI devices during the past two decades, and a large amount of fatigue test data for HFMI-treated joints has been accumulated. Recent experimental round robin exercises [2-4] have shown that several HFMI tools, namely high-frequency impact treatment (HiFIT), ultrasonic peening (UP), ultrasonic peening treatment (UPT), ultrasonic impact treatment (UIT), portable pneumatic needle peening (PPP) [5], and hammer peening on base metal [6], can provide the same degree of fatigue strength enhancement when they are used properly.

In general, although features such as removal of the original weld toe or surface finish can be expressed qualitatively as indications of complete treatment, the extent of plastic deformation, which is responsible for inducing the beneficial compressive residual stress, cannot be ascertained [7]. The IIW recommendations for HFMI treatment provide proper treatment procedures, as well as qualitative and quantitative measures of the treated area for quality control [1, 8]. As quantitative measures, the IIW states that the depth of the HFMI groove is an excellent indicator for proper treatment, and that the optimum HFMI groove is 0.2–0.6 mm deep and 3–6 mm wide, depending on the steel yield stress and the indenter size [1, 8]. In addition to control of the process and the groove profile during and after treatment, it is expected that prior prediction of the compressive residual stress imparted by the HFMI treatment would be beneficial information for a HFMI tool operator.

*: corresponding author

Residual stress around the HFMI groove can be measured non-destructively by X-ray and neutron diffraction techniques [9-12]. Furthermore, it has recently become popular to numerically simulate the HFMI process and residual stress field after the treatment [9, 10, 12-15]. These measurement and numerical simulation, while time consuming and not easy to be applied to actual structural components, are effective to clarify the compressive residual stress introduced by the HFMI treatment.

In the HFMI treatment, cylindrical indenters impact materials surface with high frequency. The kinetic energy of the accelerated indenter, which is determined by the velocity and driven mass, may be considered to be mostly converted into local plastic deformation of the impacted material and heat energy by its collision against the surface. The plastic deformation causes a change in the residual stress state and induces compressive residual stress around the impacted surface, the amount of which may be correlated with the kinetic energy of the indenter impact.

The objective of this study was to develop a method for predicting compressive residual stress induced by HFMI treatment prior to the treatment from the viewpoint of the kinetic energy of the indenter impact. Steel plates with different grades were treated under different treatment conditions, and the relationship between compressive residual stresses introduced to the plate and the kinetic energy calculated based on the recorded motion of an indenter was investigated.

2. EXPERIMENTAL PROCEDURE

2.1 Specimen

The specimens were steel plates 12 mm thick with the dimensions 200 × 170 mm. The mechanical properties of the specimens, which were taken from steel inspection certificates, are listed in Table 1. Japan Industrial Standard (JIS) grades SBHS500 and SBHS700, which are bridge high-performance steels, are newly developed high-strength steels in Japan.

Before applying the HFMI treatment, the initial residual stress in the specimens was released by annealing based on JIS Z 3700. The specimens were heated from room temperature to 595 °C for 10 hours, kept at 595 °C for 3 hours, and naturally cooled to room temperature. Residual stress measurements were performed after annealing, and it was confirmed that the initial residual stress was almost released over the entire surface of the specimen. The mean of the residual stress after annealing was -12.3 N/mm^2.

2.2 HFMI Treatment

The HFMI treatment system used in this study, shown in Fig. 1, consisted of a HFMI tool, an air compressor, and an auxiliary air tank and filter element for dehumidification. A pneumatic type HFMI device, specifically a high-frequency impact treatment (HiFIT, HiFIT Vertriebs GmbH) tool, was used for treatment. The diameter of the indenter was 3 mm. The compressed air pressure was monitored through a pressure indicator in the device and maintained at an almost constant 0.7 N/mm^2 during the treatment. The HiFIT tool impact intensity could be changed by adjusting a setting dial on the back side of the tool over a range of 0° to 960° (from lowest to highest). The impact frequency ranged from 180 to 300 Hz depending on the intensity setting.

Table 1 Mechanical properties of materials in specimens

Specimen	Material	Yield stress (N/mm^2)	Tensile strength (N/mm^2)	Elongation (%)
Steel plate	SBHS500	570	633	30
	SBHS700	823	846	24
Longitudinal attachment welded joint	Base metal (SBHS500)	587	679	30
	Deposited metal	547	619	26

Treatment patterns are shown in Fig. 2. The residual stresses before and after treatment were measured, and the residual stress introduced by the HFMI treatment was obtained. In Pattern A, a treatment process was performed over a length of 40 mm in the center of the specimen. The residual stresses were measured at locations 2, 4, 6, 8, and 10 mm away from the HFMI groove. In addition, dynamic strain measurements were performed with strain gauges during treatment, and the relationship between the strain history and the processing position was confirmed. The strains were measured at five locations alongside the groove at a distance 2 mm away from the groove. The stress and strain components targeted in this study are both in the direction perpendicular to the groove.

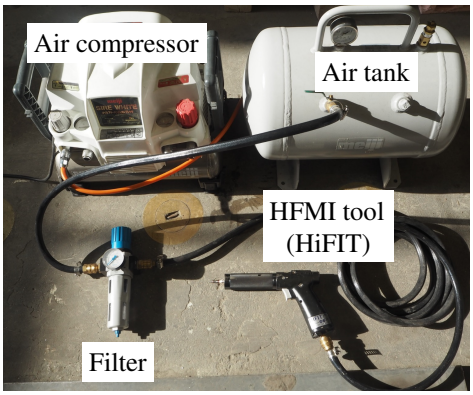

Fig. 1 HFMI treatment system

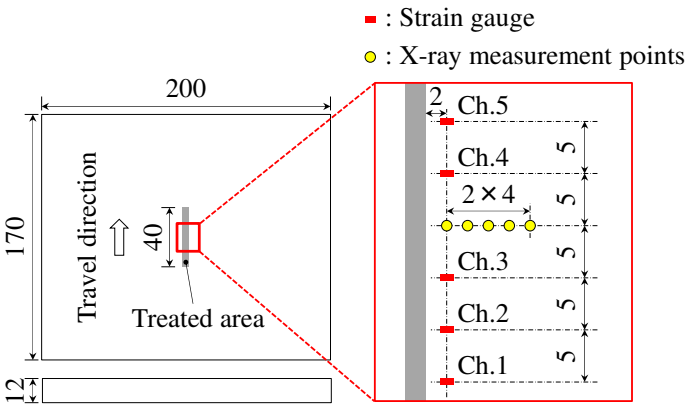

(a) Pattern A (Ch. = channel)

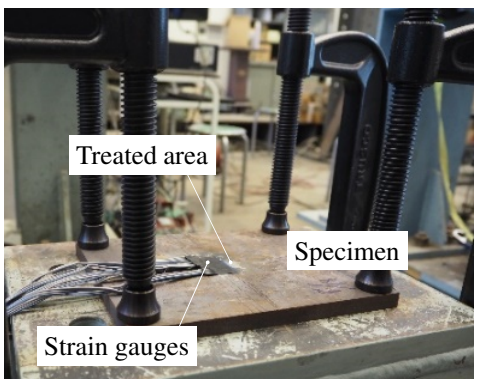

Fig. 3 Treatment setup

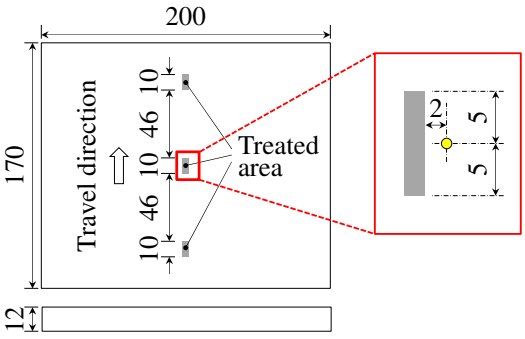

(b) Pattern B

Fig. 2 Treatment patterns (units: mm)

Table 2 Test matrix for steel plate specimens

No.	Pattern	Steel grade	Impact intensity (°)	Number of passes	Treatment length L (mm)	Treatment efficiency η (%)	Kinetic energy $E_{95\%}$ (J/mm)	Notes
1	A	SBHS 500	180	5	40	-	48.8	No indenter motion measurement
2	B		0	3	11	88.9	-	η is less than 95%
3	B		60	3	7	98.1	31.9	
4	B		60	3	13	99.4	26.2	
5	B		120	3	14	97.4	30.1	
6	B		120	3	15	99.1	40.2	
7	B		180	3	13	96.5	57.4	
8	B		180	3	15	96.4	48.0	
9	B		360	3	15	99.9	62.6	
10	B		540	3	13	98.1	89.3	
11	B		720	3	13	99.5	111.0	
12	B		180	3	16	64	-	Quality intentionally reduced
13	B		180	3	13	84.8	-	Quality intentionally reduced
14	B	SBHS 700	0	3	9	79.1	-	η is less than 95%
15	B		180	3	14	97.2	55.7	
16	B		540	3	11	99.9	135.6	
17	B	SBHS 500	180	1	11	-	18.7	No indenter motion measurement
18	B		180	2	11	-	35.1	No indenter motion measurement
19	B		180	3	12	-	51.4	No indenter motion measurement
20	B		180	5	12	-	75.0	No indenter motion measurement
21	B		180	7	11	-	102.8	No indenter motion measurement
22	B		180	9	12	-	132.8	No indenter motion measurement

In Pattern B, HFMI treatments over a length of approximately 10 mm were performed at three locations on a specimen. The results for Pattern A showed that the deformation induced by the treatment is localized, so the residual stress fields at the three locations do not affect each other. The residual stress was measured at a location 2 mm away from the groove.

The test conditions are summarized in Table 2. A total of 22 cases were tested with varying steel grade (SBHS500 and SBHS700), intensity of impact (0°–720°), number of treatment passes (1–9 passes), and treatment length (10 and 40 mm), with reference to a past study examining the effect of the HFMI process on residual stress field after the treatment [12]. Here, the number of passes means the number of times processing was repeated at the same position. Furthermore, tests were also conducted in which the tool force during processing was slightly reduced to intentionally degrade the quality of the treatment (Cases 12 and 13), in other words, the kinetic energy applied to the specimen from the device was intentionally reduced. The treatment efficiency η and kinetic energy $E_{95\%}$ shown

in the table are detailed in Section 3.3. All specimens were treated under the same constraint conditions. As shown in Fig. 3, four corners of the specimen were fixed with vises during treatment. All processing was performed by the same tool operator.

2.3 Residual Stress Measurement

Residual stresses near the HFMI groove were measured using the X-ray diffraction method (iXRD, Proto Manufacturing), which is based on the $\sin^2 \psi$ method. The collimator size was 1 mm (2 mm on the illumination surface). Before the treatment, electrolytic polishing was performed around the measurement points. After polishing, a depth gauge was used to confirm that the polishing depth was about 0.1–0.2 mm, and the depth was almost uniform at all measurement points.

The measurement was performed three times at each point, and the residual stress introduced by the HFMI treatment was obtained from the difference between the measured values before and after the treatment. The residual stress in the direction perpendicular to the HFMI groove was measured.

2.4 Motion Measurements of Indenter

To obtain the kinetic energy of the indenter during treatment, its vibrations were recorded with a high-speed camera (MEMRECAM Q1m, NAC Image Technology). As shown in Fig. 4, the motion of two targets marked around the indenter was captured and a displacement waveform was calculated from the change in distance between the targets. The camera sampling rate was set to 4,000 Hz and the motion was recorded for 2.8 seconds. The motion of the indenter when the device was idled ("blank" impact) was also captured. The pressure indicator in the device was confirmed to be almost constant at 0.7 N/mm^2 during both the blank impact and treatment process, meaning that the air pressure through the device during both blank impact and treatment was the same.

Based on the measurements, we calculated velocity waveforms for the indenter during the

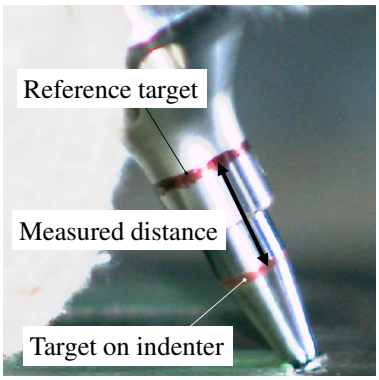

Fig. 4 Photograph of indenter operation

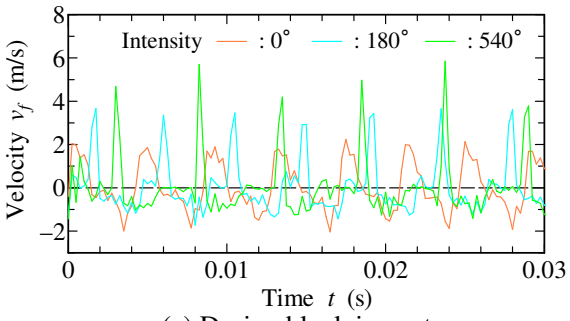

(a) During blank impact

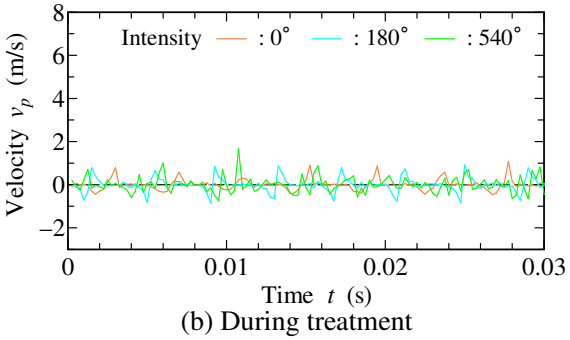

(b) During treatment

Fig. 5 Velocity waveforms

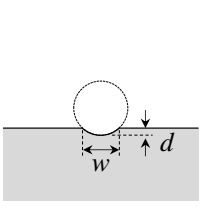

(a) Steel plate

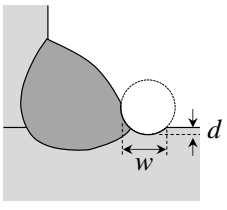

(b) Welded joint

Fig. 6 Definition of groove profile

treatment, denoted as v_p, and those during blank impact, denoted as v_f. The velocity v_f was obtained for all the impact intensities used in this study, while the velocity v_p was not measured in some tests. Fig. 5 shows examples of the measured velocity waveforms. The results for blank impact indicate that the magnitude of the velocity tends to increase as the impact intensity increases. It was also revealed that the velocity during treatment was much smaller than that during the blank impact.

2.5 Measurement of HFMI Groove Profile

Because the IIW recommendations imply that the depth of the HFMI groove is an excellent indicator of proper treatment [1, 8], HFMI groove profiles defined by the depth (d) and width (w), as shown in Fig. 6, were measured for each treated area. The measurements were performed using a replica method. Silicon replicas of HFMI grooves were sliced, and then the profile of each sample was measured by image analysis.

3. EXPERIMENTAL RESULTS

The residual stress introduced by the HFMI treatment was correlated with two indexes, namely the kinetic energy (E) applied to the specimen from the device and the cross-sectional area (A) of the HFMI groove. The definition of the kinetic energy is detailed below. The cross-sectional area was simply defined as the product of the groove depth and width ($d \times w$).

3.1 Residual Stress Distribution

The residual stress distribution after treatment was determined for Pattern A in Fig. 2 (Case 1). The treatment length was 40 mm in the center of the specimen. The impact intensity was set to 180°, and the treatment was performed with five passes. The average groove profile was 0.39 mm for depth d and 2.68 mm for width w.

Figure 7 shows the residual stress distribution introduced by the treatment. The abscissa represents the distance from the center of the HFMI groove. The average and standard deviation (SD) of the measured values are shown in the graph. A large compressive residual stress can be seen in the vicinity of the treated area, and it approaches 0 as the distance from the groove increases.

In the graph, the residual stress measured at the bottom of the groove is also shown for reference. Because the groove surface is uneven and the accuracy of the measurement at the groove bottom is not sufficient, the SD for the measurement at the groove bottom is large compared to other points. However, a large compressive residual stress is clearly introduced at the bottom of the groove. Compared to the location 2 mm away from the groove, more than twice as much residual stress, which reaches the yield stress of the material, can be introduced at the groove bottom.

In the following discussion, to evaluate the measurement accuracy, the residual stress 2 mm away from the groove, rather than the stress at the bottom of the groove, is used as an index to indicate proper treatment.

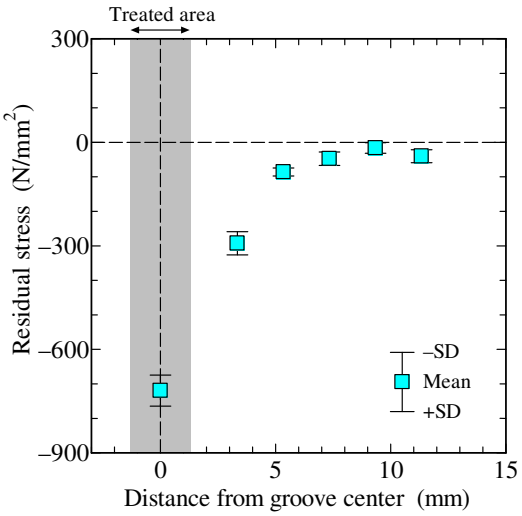

Fig. 7 Residual stress distribution in steel plate

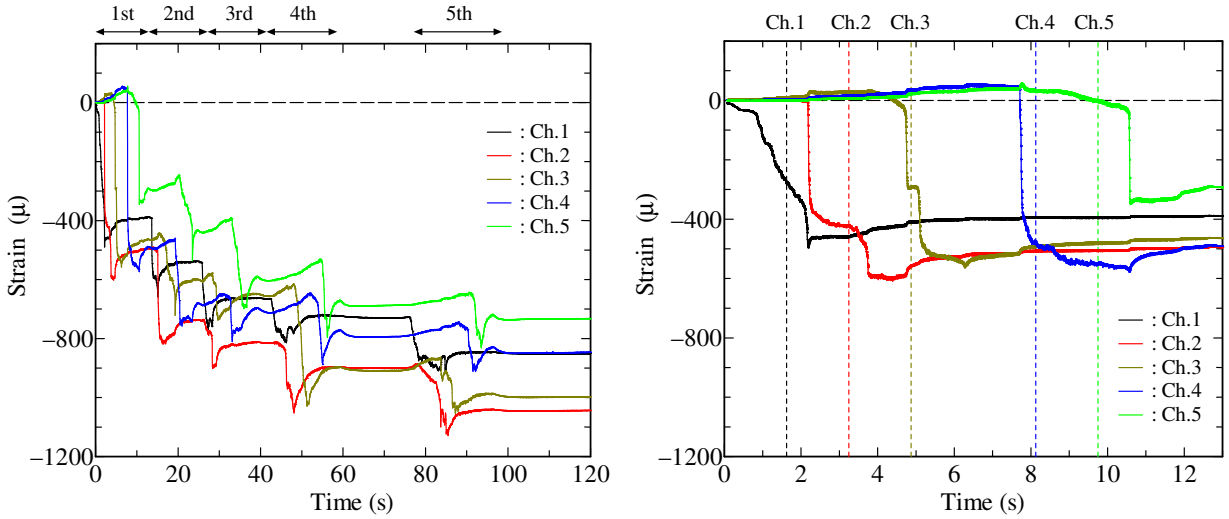

(a) 1st pass to 5th pass (b) Detail of 1st pass

Fig. 8 Strain histories during HFMI treatment

3.2 Strain Gauge Measurement

Figure 8 shows the strain fluctuation during treatment as measured by strain gauges. The strain becomes increasingly compressive during each treatment pass. However, the change in strain tends to gradually decrease as the number of passes increases.

The strain change due to the first pass is detailed in Fig. 8(b). The vertical dotted line in the graph shows the time when the indenter was near each strain gauge, as estimated from the average treatment speed (L/t). The strain tends to change significantly when the indenter passes near each strain gauge, and then remains nearly unchanged when the indenter moves away from the gauge location. Thus, it can be confirmed that the HFMI treatment influences the local residual stress field.

3.3 Definition of Kinetic Energy Applied to Steel Plate by HFMI Device

Eq. (1) shows the calculation formula for the kinetic energy per unit treatment length E applied to

the specimen by HFMI treatment. The kinetic energy ΔK due to a single impact is defined as the difference between the kinetic energy K_f obtained from the motion measurement during a blank impact and the kinetic energy K_p obtained from the motion measurement during treatment. Then, the value obtained by multiplying ΔK by the number of impacts per unit length of treatment (indenter frequency f × treatment time t / treatment length L) is defined as the kinetic energy E applied to the specimen. In addition, the ratio of ΔK and K_f is defined as the treatment efficiency η as given in Eq. (2). Here, the treatment efficiency represents the amount of kinetic energy that the indenter transfers to the specimen.

$$E = \Delta K \cdot ft/L, \tag{1a}$$

$$\Delta K = K_f - K_p = \frac{1}{2} m\left(v_f{}^2 - v_p{}^2\right), \tag{1b}$$

$$\eta = \Delta K / K_f, \tag{2}$$

where m is the mass of the indenter (0.0196 kg).

As summarized in Table 2, the treatment efficiency η was 95% or more in all cases except for the case when the impact intensity was 0° (Cases 2 and 14) and the case in which the treatment efficiency was intentionally reduced (Cases 12 and 13). This means that the treatment efficiency can be considered as 95% if the treatment was performed according to the HiFIT tool instructions. In this case, as given in Eq. (3), the kinetic energy applied to the specimen was simply calculated with only the velocity of the indenter during blank impact and the treatment efficiency η of 0.95, which is defined as $E_{95\%}$.

$$E = \eta K_f \cdot ft/L, \tag{3a}$$

$$E_{95\%} = 0.95 K_f \cdot ft/L, \tag{3b}$$

In the following discussion, $E_{95\%}$ is used as the kinetic energy applied to the specimen in all cases except for those with an impact intensity of 0° and those for which the quality was intentionally reduced (Cases 2 and 12–14). In Cases 2 and 12–14, E in Eq. (1) was used for the kinetic energy instead of $E_{95\%}$.

3.4 Residual Stress Introduced by HFMI Treatment

3.4.1 Effect of impact intensity

Fig. 9 focuses on the impact intensity to show the relationship between the applied kinetic energy $E_{95\%}$ and the introduced compressive residual stress, which is obtained in Cases 2–11. In this figure, the relationship between the residual stress and the cross-sectional area A of the groove is also shown.

As shown in Fig. 9(a), in the region where $E_{95\%}$ is less than 50 J/mm, the compressive residual stress introduced 2 mm away from the groove tends to increase as the kinetic energy increases, while the magnitude of the residual stress converges where $E_{95\%}$ is 50 J/mm or more. Here, the reason for this behavior is considered. It has been found from observations of the microstructure around a weld toe treated by ultrasonic impact treatment that the grain structure becomes finer, that is, the grain sizes change from several tens of micrometers before treatment to approximately 1 μm after treatment, leading to an improvement in the strength of the surface layer by about 15% [16].

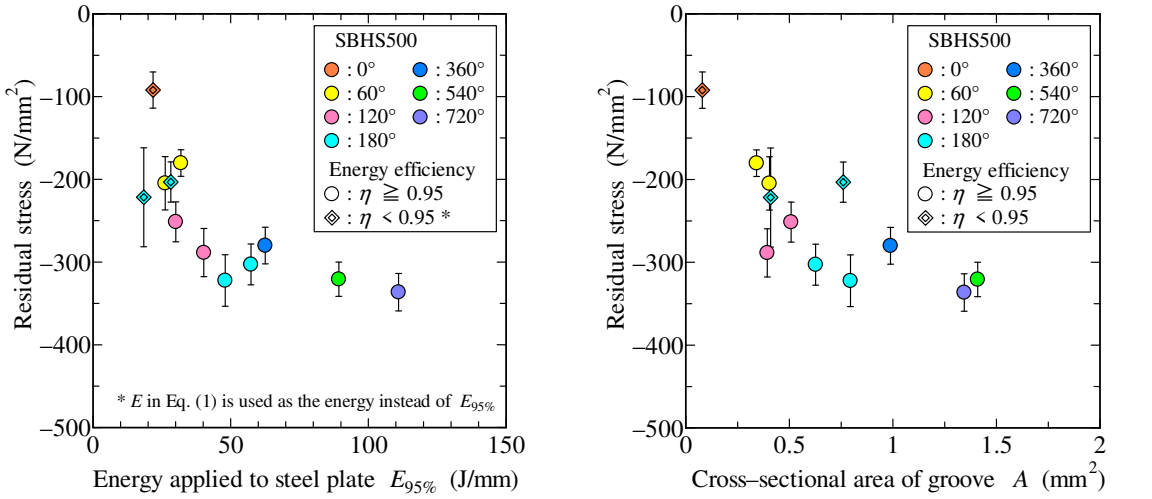

(a) Residual stress versus applied energy $E_{95\%}$ (b) Residual stress versus cross-sectional area

Fig. 9 Effect of impact intensity on introduced residual stress

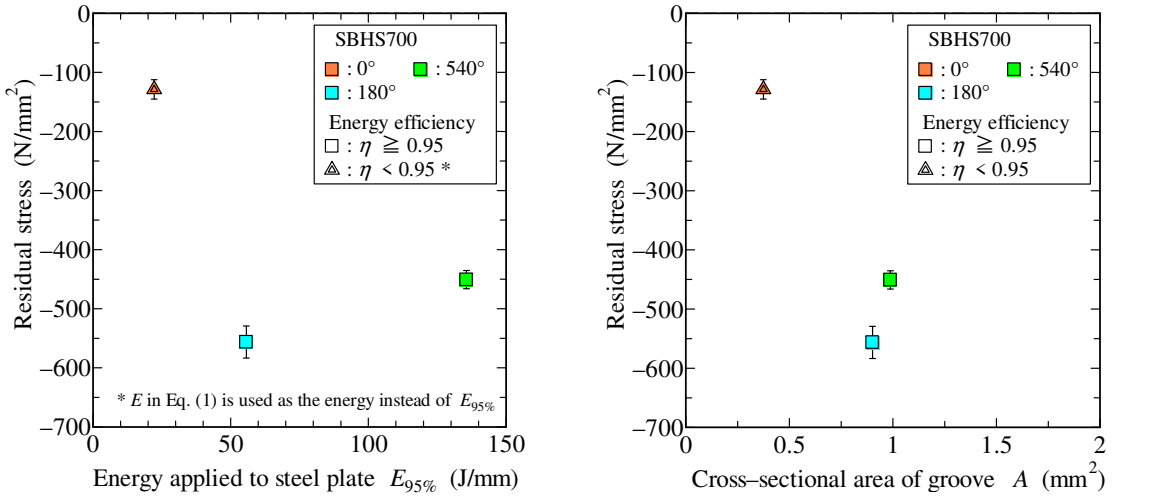

(a) Residual stress versus applied energy $E_{95\%}$ (b) Residual stress versus cross-sectional area

Fig. 10 Effect of steel grade on introduced residual stress

Furthermore, it has also been reported that when a surface is completely treated by shot peening, the surface profile is less likely to change with subsequent peening [17]. Therefore, the reason why the introduced compressive residual stress plateaus may be that the grain size reduction in the treated surface layer due to repeated impacts can improve its strength without causing more local deformation.

Fig. 9(a) also includes the results for cases in which the treatment efficiency was intentionally reduced (Cases 12 and 13). It can be seen that these results are distributed in the same region as the other results with high treatment efficiency, indicating the validity of the energy-based residual stress evaluation.

In addition, as shown in Fig. 9(b), the introduced compressive residual stress tends to increase as the cross-sectional area of the HFMI groove increases.

3.4.2 Effect of steel grade

Figure 10 shows the results for SBHS700 with different impact intensities (Cases 14–16).

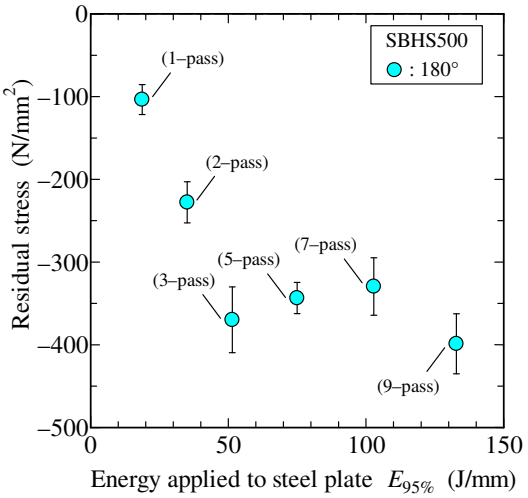

(a) Residual stress versus applied energy $E_{95\%}$

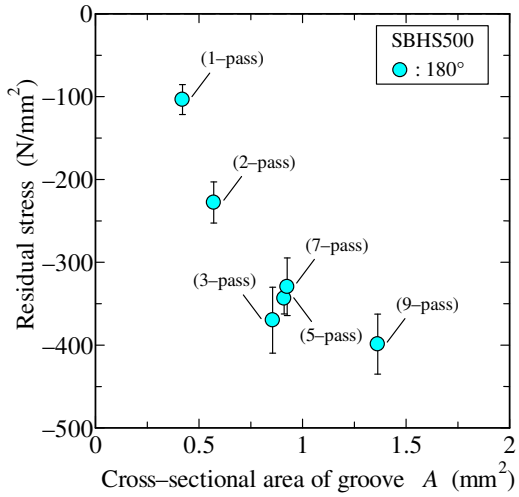

(b) Residual stress versus cross-sectional area

Fig. 11 Effect of number of treatment passes on introduced residual stress

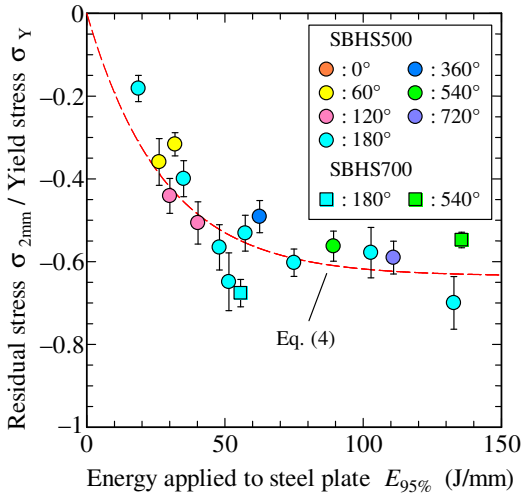

(a) Residual stress versus applied energy $E_{95\%}$

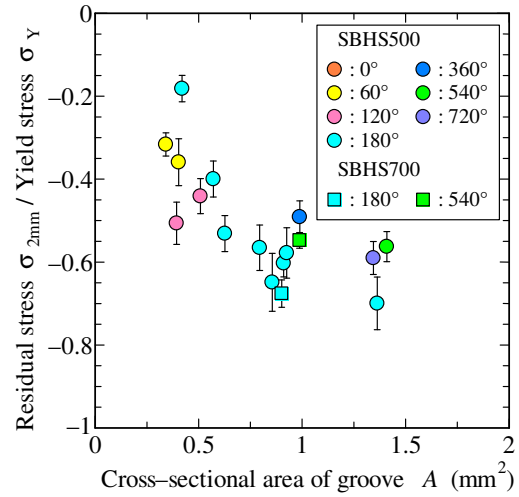

(b) Residual stress versus cross-sectional area

Fig. 12 Summary of test results for treated steel plates

Although the number of test cases is limited, the residual stress is larger compared with that in SBHS500. However, for both steel grades, the magnitude of the introduced residual stress tends to converge in the region where $E_{95\%}$ is more than 50 J/mm, as in the case of SBHS500. As shown in Fig. 10(b), a similar tendency can be observed regardless of the steel grade when compared with the cross-sectional area of the groove.

3.4.3 Effect of number of treatment passes

The results for the cases where the number of treatment passes was changed (Cases 17–22) are shown in Fig. 11. Here, the steel grade and the impact intensity are constant (SBHS500 and 180°, respectively). The compressive residual stress induced by three or more treatment passes has a tendency to become stable at about 350 to 400 N/mm^2. Moreover, the increase in the cross-sectional area of the groove tends to decrease when the number of passes is three or more.

3.4.4 Prediction of compressive residual stress

Figure 12 summarizes all the results for a treatment efficiency of 95% or more. In Fig. 12(a), the

ordinate represents the compressive residual stress 2 mm away from the HFMI groove divided by the yield stress ($\sigma_{2\,mm}/\sigma_Y$), and the abscissa represents the kinetic energy $E_{95\%}$ applied to the specimen, which is calculated using Eq. (3b) based on the assumption of a treatment efficiency of 95%. Considering that the residual stress tends to converge as the kinetic energy $E_{95\%}$ increases, the constants α and β were determined by a regression analysis that assumed the relationship to be given by an exponential function;

$$\sigma_{2mm}/\sigma_Y = \alpha\left[\exp\left(-\beta \cdot E_{95\%}\right)-1\right], \tag{4}$$

where α and β are 0.64 and 0.036, respectively, and the coefficient of determination is 0.71.

For the cross-sectional area of the groove shown in Fig. 12(b), there is a relatively large amount of scatter, and additional experiments may be needed to develop a quantitative index. A cross-sectional area of 0.8–1 mm^2 is, for example, one of the indexes for ensuring that a sufficient amount of compressive residual stress is introduced to the groove. This result is almost consistent with the proposal in a past study that used a hammer peening technique and demonstrated high fatigue strength improvement when the number of peening passes is 3 or more and the cross-sectional area of the peening groove is 1 mm^2 or more [6].

4. APPLICATION TO WELDED JOINTS

HFMI treatment controlled with the energy-based method described above was applied to welded joints, and the induced compressive residual stress and fatigue strength enhancement were investigated.

4.1 Specimen Fabrication and HFMI Treatment

Configurations and dimensions of the specimens are shown in Fig. 13. Longitudinal attachment welded joints were used for fatigue tests. The main plate and attachment were 12 mm thick, and the specimen width was 200 mm. The mechanical properties of the steel and the deposited metal used in the specimens, which were taken from steel inspection certificates, are listed in Table 1.

Carbon dioxide gas-shielded arc welding with a conventional wire 1.2 mm in diameter (JIS Z 3313 T59J1T1-1CA-N2M1-UH5) was used to fabricate the specimens. Table 3 gives the welding

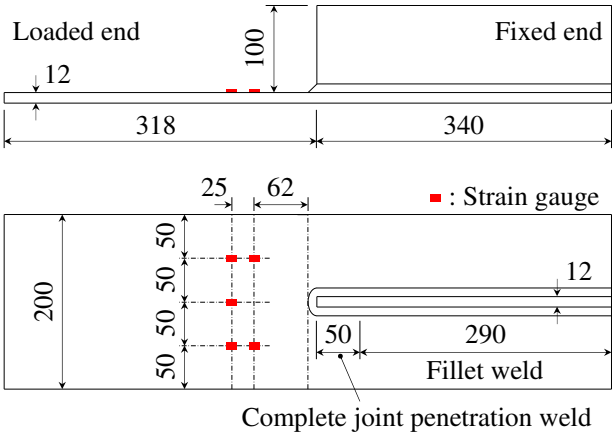

Fig. 13 Welding specimens (units: mm)

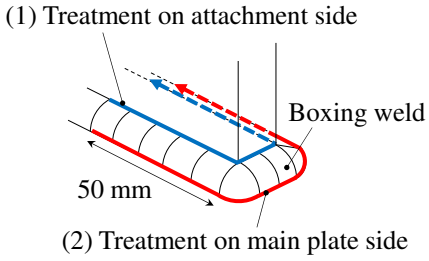

Fig. 14 HFMI treatment of boxing weld

Table 3 Welding conditions

Welding		Current	Voltage	Welding speed	Heat input
Step	Process	(A)	(V)	(cm/min)	(kJ/cm)
1	Full penetration welding	263.7	27.5	33.4	13.1
2	Boxing welding	240.7	27.7	33.6	11.9
3	Longitudinal fillet welding	247.6	27.6	35.3	11.6

conditions. To avoid root fatigue cracking from a boxing weld between the main plate and the attachment, complete joint penetration welding was applied around the boxing weld 50 mm from the attachment edge. For specimen fabrication, the attachment was first fixed to the main plate with full penetration welding with four passes, and subsequently, boxing welding with a single pass was performed to overlap the full penetration weld. Finally, the unwelded parts were connected with longitudinal fillet welding.

The boxing weld of the specimen was treated in three passes with an impact intensity of 180°. To prevent fatigue cracking from the weld toe on the attachment side, the weld toe on the attachment was also treated prior to the treatment for the weld toe on the main plate, as shown in Fig. 14. In the treatment on the main plate side, the treatment length and time per pass were approximately 138 mm and 100 seconds, respectively.

4.2 Measurement of HFMI Groove Profile

The depth (d) and width (w) of the HFMI groove, as defined in Fig. 6(b), were measured for each specimen. The measurements were performed using the replica method. Silicon replicas of boxing weld beads were sliced, and then a profile of each sample was measured by image analysis.

The distributions of groove width and depth are shown in Fig. 15. In the graph, curves indicating the groove cross-sectional areas of 0.6, 0.8, and 1 mm^2 are also shown. The average groove width, depth, and cross-sectional area are 2.41 mm, 0.37 mm, and 0.89 mm^2, respectively. Most of the groove profiles satisfy IIW recommendations, and most groove cross-sectional areas exceed 0.8 mm^2.

4.3 Residual Stress Measurement

Residual stresses near the boxing weld were measured before and after the treatment with the X-ray diffraction method (μ-X360, PULSTEC), which is based on the cos α method. The collimator size was 1 mm (2 mm on the illumination surface). The residual stress was measured in the longitudinal direction at the mid-width of the specimen starting from a location 2 mm away from the weld toe after electropolishing the specimen surface. The residual stress in the same direction as the acting stress, i.e. longitudinal direction, was measured.

Figure 16 shows the residual stress distribution in the longitudinal direction. The abscissa represents the longitudinal distance from the weld toe. Based on the treatment conditions for the longitudinal joint, the kinetic energy $E_{95\%}$ applied to the specimen calculated from Eq. (3b) is 56 J/mm. Furthermore, the compressive residual stress introduced at the location 2 mm away from the groove is estimated to be -323 N/mm^2 from Eq. (4), which is shown in the graph. In the treated specimen, a large compressive residual stress can be seen near the treated area. In addition, the

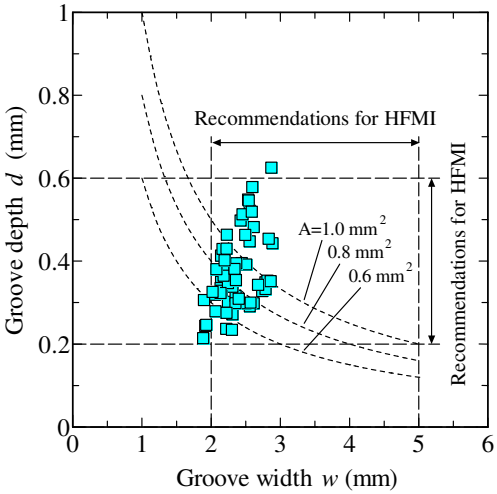

Fig. 15 HFMI groove profile

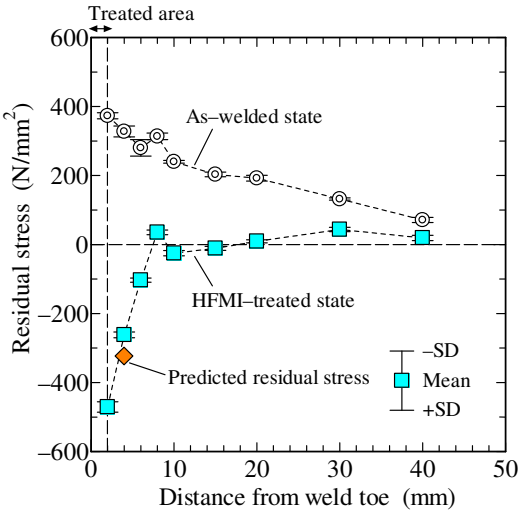

Fig. 16 Residual stress distribution in welded joint

residual stress predicted from Eqs. (3) and (4) based on the treatment conditions is almost the same as the measured values, indicating the validity of the proposed prediction formula.

4.4 Verification of Fatigue Strength Enhancement

A fatigue testing system that can generate out-of-plane bending deformation in the main plate was used for the fatigue tests [18]. One end of the main plate of the specimen was bolted to a supporting column and the other, unsupported end was subjected to cyclic loading by a vibration motor with an eccentric mass. Two stationary springs were affixed to the unsupported end of the specimen to induce a mean load in the specimen and change the stress ratio. The test was performed under a pulsating load with constant stress amplitude. The stress ratio R at the boxing weld toe was 0. The spring stiffness was set to maintain the mean stress during loading.

As shown in Fig. 13, strain gauges were placed on the main plate to monitor the stress range during the test. The nominal stress range for the specimen was determined by linearly interpolating the measured fluctuation ranges to the weld toe position. The fatigue life of the specimen, denoted as N_{10}, was defined as the number of cycles required for a crack from the weld toe to propagate 10 mm into the main plate. Cyclic loading was continued with an increased stress range when the specimen did not fail before 10 million cycles.

Fatigue test results are shown in Fig. 17, together with the results for the as-welded state and as-treated state with different HFMI tools obtained with the same type of joint and testing system [3, 4]. In the graph, the fatigue strength curves for the HFMI-treated state (in the condition of 550 N/mm^2 $\leq \sigma_Y <$ 750 N/mm^2 and $R \leq 0.15$) and for the as-welded state specified by the IIW [1, 19] are also shown. The values in parentheses represent the FAT classes of the joint in the as-welded state according to the IIW [19]. Specimens that failed by cracking from the attachment side are marked with an asterisk, and specimens that did not fail before 10 million cycles are marked with an arrow.

The results show that the fatigue strength of the specimen was significantly enhanced by the HiFIT tool, and the extent of enhancement tended to be equal to or slightly higher than that for the other HFMI tools. This means that sufficient beneficial compressive residual stress can be introduced due to the treatment and this beneficial residual stress can be predicted by the proposed method.

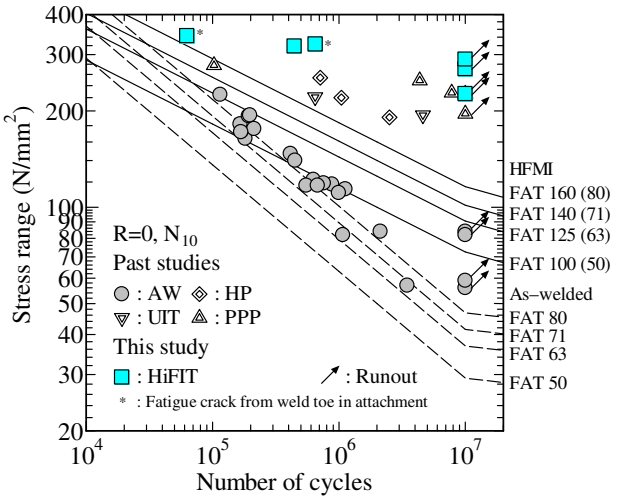

Fig. 17 Fatigue test results
(key to abbreviations: AW, as-welded; HP, hammer peening; UIT, ultrasonic impact treatment; PPP, portable pneumatic needle peening)

5. CONCLUSIONS

This study developed a method for predicting compressive residual stress introduced by HFMI treatment from the viewpoint of kinetic energy of an indenter impact. Steel plates of different grades were treated under different conditions, and the relationship between the induced compressive residual stress and the kinetic energy applied to the plate was investigated. The results obtained in this study are summarized as follows:

- This study proposed a method to estimate the kinetic energy applied to a steel plate by HFMI treatment. Moreover, it was found that the compressive residual stress introduced at a location 2 mm away from the HFMI groove can be predicted based on the estimated kinetic energy.
- It may be possible to control the amount of compressive residual stress introduced by HFMI treatment by controlling the cross-sectional area of the groove.
- Fatigue tests were conducted on longitudinal attachment weld joints treated with HFMI to achieve predicted energy levels, and sufficient fatigue strength enhancement was confirmed.

The proposed formula for predicting the compressive residual stress introduced to a plate surface by HFMI treatment was derived based mainly on the results of SBHS500. Further studies are needed to confirm its applicability to a steel with a higher static strength.

ACKNOWLEDGMENTS

The authors gratefully express their sincere gratitude to Dr. Ono and Mr. Inoue at Japan Construction Method and Machinery Research Institute for high-speed camera measurements, and to Mr. Yoshimine at Nippon Sharyo, Ltd., for fabricating the specimens. In addition, the authors wish to thank Mr. Neher at HiFIT Vertriebs GmbH for his kind support of the HiFIT tool. The authors would also like to thank Dr. Anami at Shibaura Institute of Technology and Dr. Uchida at Hosei University for useful discussions.

FUNDING

This work was partially supported by the Japan Iron and Steel Federation.

DECLARATIONS

Conflict of interest: The authors declare no competing interests.

REFERENCES

[1] G.B. Marquis and Z. Barsoum (2016) IIW recommendations for the HFMI treatment for improving the fatigue strength of welded joints, *Springer*, Singapore.

[2] H.C. Yildirim and G.B. Marquis (2013) A round robin study of high-frequency mechanical impact (HFMI)-treated welded joints subjected to variable amplitude loading, *Welding in the World*, Vol.57, pp.437-447.

[3] Japanese Society of Steel Construction (2018) JSSC Technical Report No.115, Tokyo. (in Japanese)

[4] Japanese Society of Steel Construction (2020) JSSC Technical Report No.120, Tokyo. (in Japanese)

[5] TOYO SEIKO CO., LTD. https://toyoseiko.co.jp/en/

[6] T. Nakano, K. Nakanishi and Y. Morikage (2015) Method of improving fatigue strength by peening on base metal and development of mechanized system, *JFE TECHNICAL REPORT*, No.20, pp.118-124.

[7] American Association of State Highway and Transportation Officials (2010) AASHTO LRFD bridge construction specifications, 3rd edition, Washington.

[8] G.B. Marquis and Z. Barsoum (2014) Fatigue strength improvement of steel structures by high-frequency mechanical impact: Proposed procedures and quality assurance guidelines, *Welding in the World*, Vol.58, pp.19-28.

[9] J. Foehrenbach, V. Hardenacke and M. Farajian (2016) High frequency mechanical impact treatment (HFMI) for the fatigue improvement: numerical and experimental investigations to describe the condition in the surface layer, *Welding in the World*, Vol.60, pp.749-755.

[10] M. Leitner, M. Khurshid and Z. Barsoum (2017) Stability of high-frequency mechanical impact (HFMI) post-treatment induced residual stress states under cyclic loading of welded steel joints, *Engineering Structures*, Vol.143, pp.589-602.

[11] J. Schubnell, P. Pontner, R.C. Wimpory, M. Farajian and V. Schulze (2020) The influence of work hardening and residual stresses on the fatigue behavior of high frequency mechanical impact treated surface layers, *International Journal of Fatigue*, Vol.134, 105450.

[12] J. Schubnell, C. Eichheimer, C. Ernould, A. Maciolek, J. Rebelo-Kornmeier and M. Farajian (2020) The influence of coverage for high frequency mechanical impact treatment of different steel grades, *Journal of Materials Processing Technology*, Vol.277, 116437.

[13] E. Mikkola, H. Remes and G. Marquis (2017) A finite element study on residual stress stability and fatigue damage in high-frequency mechanical impact (HFMI)-treated welded joint, *International Journal of Fatigue*, Vol.94, pp.16-29.

[14] C. Ernould, J. Schubnell, M. Farajian, A. Maciolek, D. Simunek, M. Leitner and M. Stoschka (2019) Application of different simulation approaches to numerically optimize high-frequency mechanical impact (HFMI) post-treatment process, *Welding in the World*, Vol.63, pp.725-738.

[15] H. Ruiz, N. Osawa and S. Rashed (2019) A practical analysis of residual stresses induced by high-frequency mechanical impact post-weld treatment, *Welding in the World*, Vol.63, pp.1255-1263.

[16] T. Nose (2008) Ultrasonic peening method for fatigue strength improvement, *Journal of the Japan Welding Society*, Vol.77, No.3, pp.210-213 (in Japanese).
[17] Japan Society of Shot Peening Technology (2018) Metal fatigue and shot peening, *TAIGA Publishing*, Tokyo (in Japanese).
[18] K. Yamada, S. Ya, B. Baik, A. Torii, T. Ojio and S. Yamada (2007) Development of a new fatigue testing machine and some fatigue tests for plate bending, *IIW documentation*, XIII-2161-07.
[19] A.F. Hobbacher (2016) Recommendations for fatigue design of welded joints and components, *Springer*, Switzerland.